ГОДИШНИК

НА

СОФИЙСКИЯ УНИВЕРСИТЕТ
„СВ. КЛИМЕНТ ОХРИДСКИ“

ФАКУЛТЕТ ПО МАТЕМАТИКА
И ИНФОРМАТИКА

КНИГА 1 – МАТЕМАТИКА И МЕХАНИКА
КНИГА 2 – ПРИЛОЖНА МАТЕМАТИКА И
ИНФОРМАТИКА

Том 90

ANNUAIRE

DE

L'UNIVERSITE DE SOFIA
„ST. KLIMENT OHRIDSKI“

FACULTE DE MATHEMATIQUES
ET INFORMATIQUE

LIVRE 1 – MATHEMATIQUES ET MECANIQUE
LIVRE 2 – MATHEMATIQUES APPLIQUEE ET
INFORMATIQUE

Tome 90

СОФИЯ • 1998

СОФИЯ • 1998

ГОДИШНИК НА СОФИЙСКИЯ УНИВЕРСИТЕТ „СВ. КЛИМЕНТ ОХРИДСКИ"
ФАКУЛТЕТ ПО МАТЕМАТИКА И ИНФОРМАТИКА
Книга 2 — Приложна математика и информатика
Том 90, 1996

ANNUAIRE DE L'UNIVERSITE DE SOFIA „ST. KLIMENT OHRIDSKI"
FACULTE DE MATHEMATIQUES ET INFORMATIQUE
Livre 2 — Mathématiques Appliquée et Informatique
Tome 90, 1996

NUMERICAL SOLUTIONS FOR STEADY FLOW PAST A CIRCULAR CYLINDER VIA THE METHOD OF VARIATIONAL IMBEDDING

CHRISTO I. CHRISTOV, ROSSITZA S. MARINOVA

A numerical investigation of the two-dimensional flow around a circular cylinder is performed using a primitive-variable approach. Steady (but unstable) solutions have been calculated up to Re = 200. The imbedding system is solved numerically by a difference scheme of splitting type. A staggered non-uniform grid is used. The obtained results are in good agreement with the available data.

Keywords: Navier-Stokes equations, viscous flow past a circular cylinder, high Reynolds numbers, method of variational imbedding, difference schemes

1991/95 Math. Subject Classification: 76D05, 76M30, 65M06

1. INTRODUCTION

The numerical treatment of high-Reynolds number viscous flows is of considerable interest for the applications because of the fact that the predominant part of the practically important flows take place either in large scales and high speeds or with small viscosity. Classical examples of such a kind are, above all, geophysical flows and flows around vehicles and vessels. The steady-state solution to Navier-Stokes (N-S) equations for high Reynolds numbers is unstable and cannot be treated as an initial value problem for the unsteady N-S equations. At the same time, the above mentioned problem is of crucial fundamental importance in the sense of answering

the question of which is the limiting pattern for the solution of N-S equations when the coefficient Re^{-1} of the highest-order derivatives approaches zero.

The problem of steady-state viscous incompressible flow past bluff bodies has over a long time received much attention, both theoretically and numerically. The circular cylinder is the simplest two-dimensional bluff body shape and the flow past it has been the subject of considerable experimental and numerical study. The flow round this shape has the attraction of being the source of intriguing transitions. Many of the numerical treatments are concerned with low Reynolds number flows. In spite of the many numerical calculations on flow past a circular cylinder, accurate results have been obtained only for Reynolds number ($\mathrm{Re} = U_\infty d/\nu$) up to about 700, see Fornberg [14, 15]. The Reynolds number Re is the governing dimensionless parameter. The cylinder diameter $d = 2a$ is the characteristic length; velocity at infinity U_∞ is the characteristic velocity; and ν is the kinematic coefficient of viscosity. Fornberg has found that the wake bubble (region of recirculating flow) has eddy length $L \propto \mathrm{Re}$, width $W \propto \sqrt{\mathrm{Re}}$ up to $\mathrm{Re} = 300$, and $W \propto \mathrm{Re}$ beyond that. Smith [18] has developed an asymptotic theory which agrees with Fornberg's results up to $\mathrm{Re} \approx 300$ only. Smith [20] and Peregrine [17] have performed theoretical work which gives a fresh interpretation of Fornberg's results. There are several differences between the theories of Smith and Peregrine, some of which are a matter of interpretation. These are unlikely to be resolved without further analysis and computational work.

The problem of viscous steady-state flow past a circular cylinder at high Reynolds numbers represents one of the classical problems in fluid mechanics. Although some agreement between theoretical, numerical and experimental results exists, there is a need for further work in all these aspects of this fundamental and classical problem. In the present paper the steady-state Navier-Stokes equations are solved using the so-called Method of Variational Imbedding.

2. BASIC EQUATIONS AND METHOD OF SOLUTION

The N-S equations are given in dimensionless form, corresponding to a cylinder of radius $r = 1$ in an uniform stream of unit magnitude with direction along the positive axis of x. Polar co-ordinates (r, φ) are used. The N-S equations governing the steady-state motion then read

$$u_r \frac{\partial u_\varphi}{\partial r} + \frac{u_\varphi}{r}\frac{\partial u_\varphi}{\partial \varphi} + \frac{u_\varphi u_r}{r} = -\frac{1}{r}\frac{\partial p}{\partial \varphi} + \frac{1}{\mathrm{Re}}\left[Du_\varphi + \frac{2}{r^2}\frac{\partial u_r}{\partial \varphi}\right], \tag{2.1}$$

$$u_r \frac{\partial u_r}{\partial r} + \frac{u_\varphi}{r}\frac{\partial u_r}{\partial \varphi} - \frac{u_\varphi^2}{r} = -\frac{\partial p}{\partial r} + \frac{1}{\mathrm{Re}}\left[Du_r - \frac{2}{r^2}\frac{\partial u_\varphi}{\partial \varphi}\right], \tag{2.2}$$

$$\frac{\partial u_r}{\partial r} + \frac{u_r}{r} + \frac{1}{r}\frac{\partial u_\varphi}{\partial \varphi} = 0, \tag{2.3}$$

where $u_r = u(r,\varphi)$ and $u_\varphi = v(r,\varphi)$ are the velocity components parallel respectively to the polar axes r and φ; $p = p(r,\varphi)$ is the pressure. Respectively,

$$D \equiv \frac{\partial^2}{\partial r^2} + \frac{1}{r}\frac{\partial}{\partial r} - \frac{1}{r^2} + \frac{1}{r^2}\frac{\partial^2}{\partial \varphi^2}$$

is the so-called *Stokesian*.

In terms of dimensionless variables, the cylinder surface is represented by $r = 1$, while the velocity at infinity — by unity.

The boundary conditions reflect the non-slipping at the cylinder surface

$$u_r(1,\varphi) = u_\varphi(1,\varphi) = 0, \tag{2.4}$$

on the one hand, and the asymptotic matching with the uniform outer flow at infinity, on the other. Numerically one has to pose the asymptotic condition at a certain large enough value of the radial co-ordinate, called "actual infinity," say, r_∞. Then the dimensionless boundary conditions read

$$u_r(r_\infty,\varphi) = \cos\varphi, \quad u_\varphi(r_\infty,\varphi) = -\sin\varphi. \tag{2.5}$$

Due to the obvious flow symmetry with respect to the line $\varphi = 0, \pi$, the computational domain may be reduced to $0 \le \varphi \le \pi$, $r \ge 1$ and additional boundary conditions on the lines $\varphi = 0$ and $\varphi = \pi$ are added to acknowledge the mentioned symmetry, namely:

$$u_\varphi = \frac{\partial u_r}{\partial \varphi} = 0 \quad \text{for} \quad \varphi = 0, \pi. \tag{2.6}$$

2.1. APPLYING THE METHOD OF VARIATIONAL IMBEDDING

For tackling inverse and incorrect problems, Christov [4 - 6] has developed the already mentioned Method of Variational Imbedding (MVI) which is a special implementation of the Least Square Method to ODE and PDE.

Consider the imbedding functional

$$\mathcal{J} = \int_0^\pi \int_1^\infty \left(\Phi^2 + \Omega^2 + X^2\right) r\, dr d\varphi, \tag{2.7}$$

where

$$\Phi = u_r\frac{\partial u_\varphi}{\partial r} + \frac{u_\varphi}{r}\frac{\partial u_\varphi}{\partial \varphi} + \frac{u_\varphi u_r}{r} + \frac{1}{r}\frac{\partial p}{\partial \varphi} - \frac{1}{\mathrm{Re}}\left(Du_\varphi + \frac{2}{r^2}\frac{\partial u_r}{\partial \varphi}\right),$$

$$\Omega = u_r\frac{\partial u_r}{\partial r} + \frac{u_\varphi}{r}\frac{\partial u_r}{\partial \varphi} - \frac{u_\varphi^2}{r} + \frac{\partial p}{\partial r} - \frac{1}{\mathrm{Re}}\left(Du_r - \frac{2}{r^2}\frac{\partial u_\varphi}{\partial \varphi}\right),$$

$$X = \frac{\partial u_r}{\partial r} + \frac{u_r}{r} + \frac{1}{r}\frac{\partial u_\varphi}{\partial \varphi}.$$

As far as the boundary value problem for the N-S equations possesses a solution, then the global minimum of the functional (2.7) is equal to zero, which is the value the functional assumes on the solutions of N-S. This allows us to seek a local minimum of the functional $\mathcal{J}$ and to check afterwards whether this is the global minimum.

The necessary conditions for minimizing of a functional are the Euler-Lagrange equations (see [8]). After some simplification these equations of Euler-Lagrange for the velocity components and pressure take the form of a conjugated system for Φ, u_φ, Ω, u_r and p:

$$\frac{1}{\mathrm{Re}}\left(D\Phi + \frac{2}{r^2}\frac{\partial \Omega}{\partial \varphi}\right) + \left(u_r\frac{\partial \Phi}{\partial r} + \frac{u_\varphi}{r}\frac{\partial \Phi}{\partial \varphi} + \frac{2u_\varphi \Omega}{r} + \frac{1}{r}\frac{\partial \mathrm{X}}{\partial \varphi}\right) + \Phi\frac{\partial u_r}{\partial r} - \frac{\Omega}{r}\frac{\partial u_r}{\partial \varphi} = 0,$$

$$\frac{1}{\mathrm{Re}}\left(Du_\varphi + \frac{2}{r^2}\frac{\partial u_r}{\partial \varphi}\right) - \left(u_r\frac{\partial u_\varphi}{\partial r} + \frac{u_\varphi}{r}\frac{\partial u_\varphi}{\partial \varphi} + \frac{u_\varphi u_r}{r} + \frac{1}{r}\frac{\partial p}{\partial \varphi}\right) + \Phi = 0,$$

$$\frac{1}{\mathrm{Re}}\left(D\Omega - \frac{2}{r^2}\frac{\partial \Phi}{\partial \varphi}\right) + \left(u_r\frac{\partial \Omega}{\partial r} + \frac{u_\varphi}{r}\frac{\partial \Omega}{\partial \varphi} - \frac{u_\varphi \Phi}{r} + \frac{\partial \mathrm{X}}{\partial r}\right) - \Phi\frac{\partial u_\varphi}{\partial r} - \Omega\frac{\partial u_r}{\partial r} = 0,$$

$$\frac{1}{\mathrm{Re}}\left(Du_r - \frac{2}{r^2}\frac{\partial u_\varphi}{\partial \varphi}\right) - \left(u_r\frac{\partial u_r}{\partial r} + \frac{u_\varphi}{r}\frac{\partial u_r}{\partial \varphi} - \frac{u_\varphi^2}{r} + \frac{\partial p}{\partial r}\right) + \Omega = 0,$$

$$\Delta p - \frac{2}{r}\left(\frac{\partial u_\varphi}{\partial \varphi}\frac{\partial u_r}{\partial r} - \frac{\partial u_\varphi}{\partial r}\frac{\partial u_r}{\partial \varphi} + u_\varphi\frac{\partial u_\varphi}{\partial r} + u_r\frac{\partial u_r}{\partial r}\right) = 0.$$

All five equations above are of elliptic type and of second order on each boundary point. Therefore, five boundary conditions are needed. We already posed two of them when formulating the problem, see Eqs. (2.4) — (2.6). The remaining three are the natural conditions for minimization of the functional (2.7), which are nothing else but $\Phi = \Omega = \mathrm{X} = 0$. From the continuity equation $\mathrm{X} = 0$ we have $\partial u_r/\partial r = 0$ at the boundaries $r = 1$ and $r = r_\infty$. Respectively, the symmetry conditions at the lines of symmetry $\varphi = 0, \pi$ are $\partial p/\partial \varphi = 0$, which is equivalent to the condition on the function $u_\varphi(r, \varphi)$ at the same lines, namely $-\partial^2 u_\varphi/\partial \varphi^2 = 0$. Thus we have a correctly posed boundary problem for the set of functions we are looking for.

It is clear that if we find a solution of the imbedding system for which Φ and Ω are equal to zero, then u_φ, u_r and p form the solution of the original problem.

Here we consider the same problem that was outlined in [8]. The difference is that we treat the Imbedding system differently. In [8] the autors have solved numerically the Imbedding system of Euler–Lagrange equations for functions u_φ, u_r which are of forth order, and pressure equation for p of second order. This system looks apparently much more complicated (together with boundary conditions) than the system of five equations for Φ, u_φ, Ω, u_r and p.

We introduce the notations (E is the unitary operator)

$$\vec{\theta} = \begin{pmatrix} \Phi \\ u_\varphi \\ \Omega \\ u_r \\ p \end{pmatrix}, \quad F^{\vec{\theta}} = \begin{pmatrix} F^\Phi \\ F^{u_\varphi} \\ F^\Omega \\ F^{u_r} \\ F^p \end{pmatrix}, \quad I = \begin{pmatrix} E & 0 & 0 & 0 & 0 \\ 0 & E & 0 & 0 & 0 \\ 0 & 0 & E & 0 & 0 \\ 0 & 0 & 0 & E & 0 \\ 0 & 0 & 0 & 0 & E \end{pmatrix},$$

where

$$F^\Phi = \frac{2}{\mathrm{Re}\cdot r^2}\frac{\partial \Omega}{\partial \varphi} + u_r\frac{\partial \Phi}{\partial r} + \frac{u_\varphi}{r}\frac{\partial \Phi}{\partial \varphi} + \frac{2u_\varphi \Omega}{r} + \frac{1}{r}\frac{\partial X}{\partial \varphi} + \Phi\frac{\partial u_r}{\partial r} - \frac{\Omega}{r}\frac{\partial u_r}{\partial \varphi},$$

$$F^{u_\varphi} = \frac{2}{\mathrm{Re}\cdot r^2}\frac{\partial u_r}{\partial \varphi} - \left(u_r\frac{\partial u_\varphi}{\partial r} + \frac{u_\varphi}{r}\frac{\partial u_\varphi}{\partial \varphi} + \frac{u_\varphi u_r}{r}\right),$$

$$F^\Omega = -\frac{2}{\mathrm{Re}\cdot r^2}\frac{\partial \Phi}{\partial \varphi} + u_r\frac{\partial \Omega}{\partial r} + \frac{u_\varphi}{r}\frac{\partial \Omega}{\partial \varphi} - \frac{u_\varphi \Phi}{r} + \frac{\partial X}{\partial r} - \Phi\frac{\partial u_\varphi}{\partial r} - \Omega\frac{\partial u_r}{\partial r},$$

$$F^{u_r} = -\frac{2}{\mathrm{Re}\cdot r^2}\frac{\partial u_\varphi}{\partial \varphi} - \left(u_r\frac{\partial u_r}{\partial r} + \frac{u_\varphi}{r}\frac{\partial u_r}{\partial \varphi} - \frac{u_\varphi^2}{r}\right),$$

$$F^p = -\frac{2}{r}\left(\frac{\partial u_\varphi}{\partial \varphi}\frac{\partial u_r}{\partial r} - \frac{\partial u_\varphi}{\partial r}\frac{\partial u_r}{\partial \varphi} + u_\varphi\frac{\partial u_\varphi}{\partial r} + u_r\frac{\partial u_r}{\partial r}\right),$$

$$\Lambda_{rr} = \frac{1}{\mathrm{Re}}\left(\frac{1}{r}\frac{\partial}{\partial r}r\frac{\partial}{\partial r} - \frac{1}{r^2}\right), \quad \Lambda_{\varphi\varphi} = \frac{1}{\mathrm{Re}\cdot r^2}\frac{\partial^2}{\partial \varphi^2}, \quad \Lambda_r = \frac{\partial}{\partial r}, \quad \Lambda_\varphi = \frac{1}{r}\frac{\partial}{\partial \varphi},$$

$$\Lambda_{rr}^{[p]} = \frac{1}{r}\frac{\partial}{\partial r}r\frac{\partial}{\partial r}, \quad \Lambda_{\varphi\varphi}^{[p]} = \frac{1}{r^2}\frac{\partial^2}{\partial \varphi^2}.$$

Upon denoting by

$$\Lambda_1 = \begin{pmatrix} \Lambda_{rr} & 0 & 0 & 0 & 0 \\ \frac{1}{2}E & \Lambda_{rr} & 0 & 0 & 0 \\ 0 & 0 & \Lambda_{rr} & 0 & 0 \\ 0 & 0 & \frac{1}{2}E & \Lambda_{rr} & -\Lambda_r \\ 0 & 0 & 0 & 0 & \Lambda_{rr}^{[p]} \end{pmatrix}$$

and

$$\Lambda_2 = \begin{pmatrix} \Lambda_{\varphi\varphi} & 0 & 0 & 0 & 0 \\ \frac{1}{2}E & \Lambda_{\varphi\varphi} & 0 & 0 & -\Lambda_\varphi \\ 0 & 0 & \Lambda_{\varphi\varphi} & 0 & 0 \\ 0 & 0 & \frac{1}{2}E & \Lambda_{\varphi\varphi} & 0 \\ 0 & 0 & 0 & 0 & \Lambda_{\varphi\varphi}^{[p]} \end{pmatrix},$$

we render the equations for Φ, u_φ, Ω, u_r and p to the following vectorial form for $\vec{\theta}$:

$$(\Lambda_1 + \Lambda_2)\vec{\theta} + F^{\vec{\theta}} = 0. \tag{2.8}$$

Upon adding derivatives with respect to a fictitios time t, we get

$$\frac{\partial \vec{\theta}}{\partial t} = (\Lambda_1 + \Lambda_2)\vec{\theta} + F^{\vec{\theta}}. \tag{2.9}$$

Note that in the physically unsteady case the time derivatives are present only in the equations for the velocity components (the original system is not of *Cauchy-Covalewska* type).

2.3. THE SPLITTING SCHEME

The system under consideration is non-linear. It can be solved by means of an iterational process in which at each stage the equations are linearized. In the present work we make use of the iterative procedure based on the co-ordinate-splitting method because of its computational efficiency. We employ the method of fractional steps, namely the second scheme of Douglas and Rachford [12], sometimes called the scheme of "stabilizing correction" [22]. The stabilizing correction scheme reads (τ is the increment of the fictitious time)

$$\frac{\vec{\theta}^{n+\frac{1}{2}} - \vec{\theta}^n}{\tau} = \Lambda_1\vec{\theta}^{n+\frac{1}{2}} + \Lambda_2\vec{\theta}^n + F^{\vec{\theta}^n}, \qquad \frac{\vec{\theta}^{n+1} - \vec{\theta}^{n+\frac{1}{2}}}{\tau} = \Lambda_2\vec{\theta}^{n+1} - \Lambda_2\vec{\theta}^n,$$

or, which is the same,

$$(I - \tau\Lambda_1)\vec{\theta}^{n+\frac{1}{2}} = (I + \tau\Lambda_2)\vec{\theta}^n + \tau F^{\vec{\theta}^n}, \quad (I - \tau\Lambda_2)\vec{\theta}^{n+1} = \vec{\theta}^{n+\frac{1}{2}} - \tau\Lambda_2\vec{\theta}^n.$$

The approximation with respect to fictitious time can be assessed after excluding the half time-step variable $\vec{\theta}^{n+\frac{1}{2}}$. After some obvious manipulations, we obtain the equation

$$(I + \tau^2\Lambda_1\Lambda_2)\frac{\vec{\theta}^{n+1} - \vec{\theta}^n}{\tau} = (\Lambda_1 + \Lambda_2)\vec{\theta}^{n+1} + F^{\vec{\theta}^n}. \tag{2.10}$$

The splitting scheme is implicit for the linear terms and explicit for the non-linear convective terms.

2.4. GRID PATTERN AND APPROXIMATIONS

The flow field shows a mixture of different scales for high Re. There is a thin boundary layer close to the body, which separates and extends downstream. Neither Cartesian nor polar co-ordinate systems are adequate enough for describing the topology of the flow when the separation takes place. These problems are aggravated with the increase of the Reynolds number. The usual polar co-ordinate

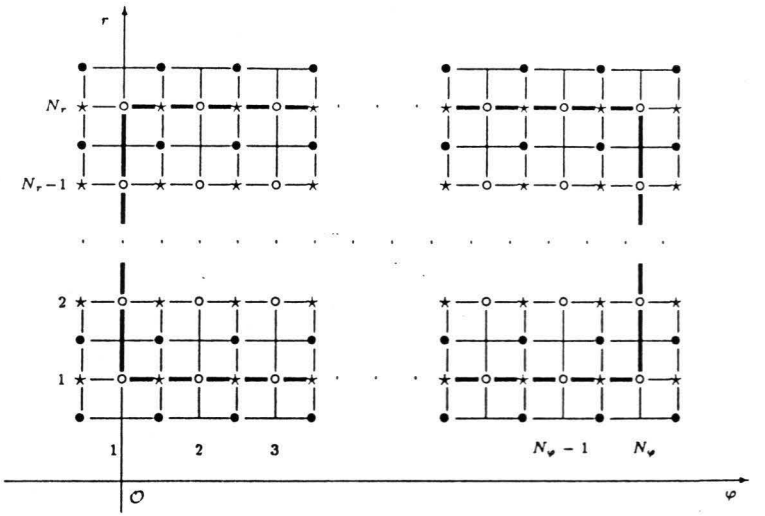

Fig. 1. Grid pattern

system, dense enough to resolve the wake far out, will be very wasteful in other directions. For this reason our mesh labelled by 'o' is chosen to be non-uniform. The spacings are given by

$$h_r = \frac{R-1}{N_r - 1}, \quad h_\varphi = \frac{\pi}{N_\varphi - 1},$$

where N_r stands for the number of points in the direction r and N_φ — in the direction φ, respectively. The mesh is staggered for p in direction φ. For u_r and Ω it is staggered in both directions. In Fig. 1 the mesh is depicted, where the thick lines represent the borders of the region of computations. The co-ordinates of a point of the mesh are defined as follows:

$$r_i = \exp[(i-1)h_r], \ \varphi_j = \frac{1}{\pi}[(j-1)h_\varphi]^2, \text{ where } i = 1, \ldots, N_r; \ j = 1, \ldots, N_\varphi.$$

The points in Fig. 1, which are labelled by 'o', are those where the functions u_φ and Φ are calculated. The pressure is calculated in the points labelled by '$\star$', and functions u_r and Ω are calculated in the grid point labelled by '$\bullet$'.

We employ the following two-point and three-point approximations for the first and second derivatives (equivalent to the central differences scheme on uniform mesh). The derivatives are approximated as

$$\left.\frac{\partial u}{\partial x}\right|_{i-\frac{1}{2}} \approx \frac{u_i - u_{i-1}}{h_{i-1}},$$

$$\left.\frac{\partial u}{\partial x}\right|_i \approx \frac{h_{i-1}}{h_i(h_i+h_{i-1})}u_{i+1} + \frac{h_i - h_{i-1}}{h_i h_{i-1}}u_i - \frac{h_i}{h_{i-1}(h_i+h_{i-1})}u_{i-1},$$

$$\left.\frac{\partial^2 u}{\partial x^2}\right|_i \approx \frac{2}{h_i + h_{i-1}}\left[\frac{u_{i+1}-u_i}{h_i} - \frac{u_i - u_{i-1}}{h_{i-1}}\right],$$

where u stands for Φ, u_φ, Ω, u_r or p and x stands for r or φ. Respectively, h_{i-1} and h_i are the values of the spacing on the left or on the right from the reference point (Fig. 2).

Fig. 2. A point of the non-uniform mesh

The staggered mesh allows to use second order approximations for the boundary conditions. All boundary conditions are imposed implicitly.

2.5. IMPLEMENTATION OF THE SCHEME

The algebraic problem is coupled with the difference approximations of the boundary conditions. The boundary conditions for the pressure equation stem from the additional condition on function u_r from the continuity equation. The idea consists in treating the system for different half-time steps as conjugated (see [19, 2]). On the first half-time step (the operators with derivatives with respect to r) we solve the equations for the "vector" $\{\Phi, u_\varphi\}$. Respectively, the equations for the "vector" $\{\Omega, u_r, p\}$ are solved simultaneously. On the second half-time step (derivatives with respect to φ) the respective equations for the vectors $\{p, u_\varphi, \Phi\}$ and $\{u_r, \Omega\}$ are solved. The arguments for selecting the "pairs" and "triplets" of equations are obvious: Φ enters the equation for u_φ, while Ω enters the equation for u_r. The resulting systems are either five- or seven-diagonal and can be treated by the solver described in [7]. The method of the so-called non-monotonous *progonka* is a kind of Gaussian elimination with pivoting and it is highly efficient for multidiagonal cases. The solution algorithm allows for complete coupling of the boundary conditions.

We solve the system governing the functions $\Phi(r,\varphi)$, $u_\varphi(r,\varphi)$, $\Omega(r,\varphi)$, $u_r(r,\varphi)$ and $p(r,\varphi)$ in the following iterational manner:

(i) The initial conditions Φ^0, u_φ^0, Ω^0, u_r^0, p^0 for small Reynolds numbers ($\mathrm{Re} \approx 2 \div 4$) are defined as

$$\Phi|_{i,j} = 0,\ u_\varphi|_{i,j} = \frac{r_i - 1}{r_\infty - 1}\cos\varphi_j,\ \Omega|_{i,j} = 0,\ u_r|_{i,j} = \frac{r_i - 1}{r_\infty - 1}\sin\varphi_j,\ p|_{i,j} = 0.$$

For larger values of Reynolds number the solution for the closest smaller Re is used as the initial condition for the iterations for the current Re.

The counter of time steps is set $n = 0$;

(ii) On the first half-step for the line $\varphi = \varphi_j$ we solve two systems for the unknowns $\Phi^{n+\frac{1}{2}}$, $u_\varphi^{n+\frac{1}{2}}$, $\Omega^{n+\frac{1}{2}}$, $u_r^{n+\frac{1}{2}}$ and $p^{n+\frac{1}{2}}$ — with a seven-diagonal matrix for $\{\Omega, u_r, p\}$ and a five-diagonal matrix for $\{\Phi, u_\varphi\}$;

(iii) Similarly, for the vectors Φ^{n+1}, u_φ^{n+1}, Ω^{n+1}, u_r^{n+1} and p^{n+1}, we solve for the lines $r = r_i$ on the second half-step two systems — with a five-diagonal matrix for $\{\Omega, u_r\}$ and a seven-diagonal matrix for $\{\Phi, u_\varphi, p\}$;

(iv) The norm of the difference between two consecutive iterations $(n+1)$ and (n) (time steps with respect to fictitious time)

$$\max_{i,j} |\vec{\theta}^{n+1} - \vec{\theta}^{n}|$$

is calculated. If this norm is lesser than a prior prescribed value, then the calculations are terminated. Otherwise the index of iterations is stepped up $n := n + 1$ and the algorithm is returned to step (ii).

3. RESULTS AND DISCUSSION

In order to assess the approximation of the proposed scheme and the performance of the algorithm, a number of numerical experiments have been conducted.

The accuracy of the developed here difference scheme and algorithm is checked with the mandatory tests involving different increments of the fictitious time τ and mesh parameters: N_φ, N_r and r_∞.

First of all, we check that the approximation of the steady-state solution does not depend of the fictitious time increment of the splitting scheme. Theoretically, it follows from equation (2.10) and provides a good check for the correctness of the algorithm if it is respected in practice. We have calculated the flow with $\mathrm{Re} = 40$ with three different fictitious-time increments: $\tau = 0.1, 0.01, 0.001$. We have found that the iterative solution of the steady-state problem does not depend on the magnitude of the time increment τ.

The second important verification is the spatial approximation of the scheme. We have conducted a number of calculations with different values of mesh parameters and verified the practical convergence and the approximation of the difference scheme. In Table 1 and Table 2 we present the obtained numerical results for some parameters like positions of separation point φ_{sep} from the rear stagnation point, difference between the pressure at front and at rear of stagnation point. The values of the drag coefficient C_D are computed from

$$C_D = -2 \int_0^{\pi} p(1, \varphi) \cos\varphi \, d\varphi - \frac{4}{\mathrm{Re}} \int_0^{\pi} \left. \frac{\partial u_\varphi}{\partial r} \right|_{r=1} \sin\varphi \, d\varphi.$$

The first term on the right gives the pressure drag coefficient and the second — the friction drag coefficient. In these tests Re = 100, $r_\infty \approx 53$. For $N_\varphi = 125$ and $N_\varphi = 195$ the difference between the present results for φ_{sep} and $p(1,\pi) - p(1,0)$ is indistinguishable within the accuracy of calculations with ordinary precision. But for $N_r = 126$ and $N_r = 161$ the flow picture changes significantly. These calculations illustrate the convergence of the difference approximation to the solution of the differential problem under study.

TABLE 1. Results of calculation for different N_φ, Re = 100, $N_r = 126$ and $r_\infty \approx 53$

N_φ	φsep	C_D	$p(1,\pi) - p(1,0)$
100	1.013	0.89820	0.56900
125	1.031	0.89289	0.59805
195	1.031	0.89081	0.59805

TABLE 2. Results of calculation for different N_r, Re = 100, $N_\varphi = 126$ and $r_\infty \approx 53$

N_r	φsep	C_D	$p(1,\pi) - p(1,0)$
126	1.031	0.89289	0.59805
161	1.049	0.94539	0.63609
199	1.065	0.96055	0.64400

The values of r_∞ are obtained as the results of experience [13, 11].

We have successful calculations for $2 \leq \text{Re} \leq 200$. The numbers of grid points N_φ and N_r cannot be very large (although it is desired) due to computer limitations. The tests have shown that for $\text{Re} \leq 100$ the mesh size with $N_\varphi = 150$, $N_r = 251$, $r_\infty \approx 88$ is probably safe. The calculations at Re = 200 presented bellow are carried out by using the mesh size $N_\varphi = 125$, $N_r = 199$, $r_\infty \approx 80$.

Some of our results along with the results of other authors are given in Table 3 for comparison. The values of C_D, L and $p(1,\pi) - p(1,0)$ for $\text{Re} = 20, 40, 50, 100$ are in good agreement with those of Fornberg [13] and reasonably agree with those of Takami and Keller [21] and Dennis and Chang [11].

TABLE 3. Calculated values for C_D, L and $p(1,\pi) - p(1,0)$

Ref.	Re	C_D	L	$p(1,\pi) - p(1,0)$
[21]	20	2.003	2.87	
	40	1.536	5.65	
	50	1.418	7.10	
[11]	20	2.045	2.88	0.9290
	40	1.522	5.69	0.8265
	100	1.056	14.11	0.7265
[13]	20	2.000	2.82	0.910
	40	1.498	5.48	0.801
	100	1.060	13.20	0.693
	200	0.831	26.20	0.589
Present work	20	2.0095	2.84	0.9215
	40	1.4877	5.47	0.8163
	50	1.3470	6.61	0.7843
	100	1.0052	13.33	0.6956
	200	0.6769	17.81	0.4740

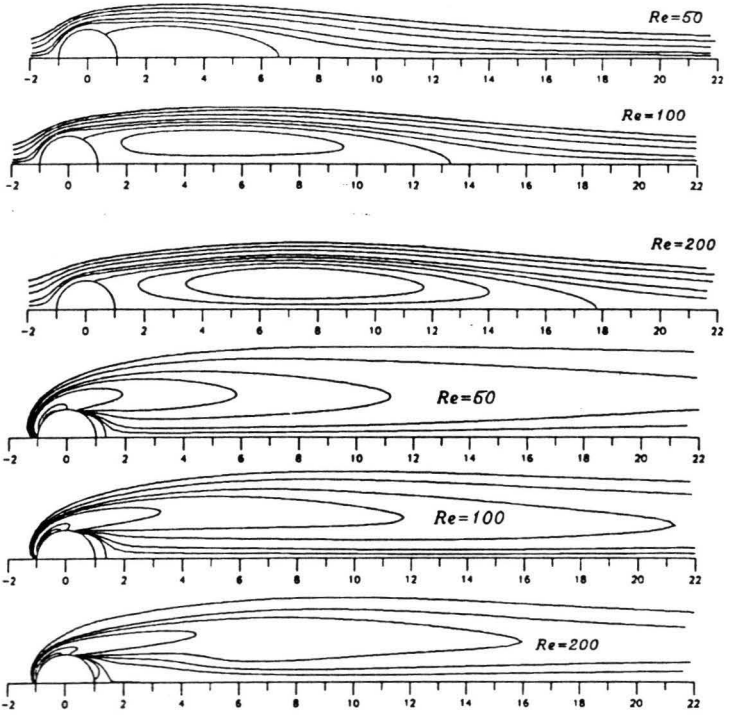

Fig. 3. Streamlines and vorticity fields

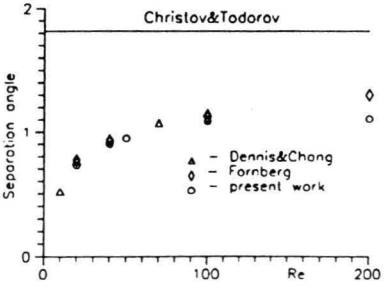

Fig. 4. The separation angle

Streamlines and vorticity isolines of the flow for Reynolds numbers 50, 100 and 200 are shown in Fig. 3. For the stream function the contour values, starting from the top, are $\{0.4,\ 0.3,\ 0.2,\ 0.1,\ 0.05\}$; enclosed streamlines, starting from the centre, are $\{-0.1,\ -0.05,\ 0\}$, and for the vorticity the contour values are $\{0.1,\ 0,\ -0.2,\ -0.4,\ -0.6,\ -1,\ -3,\ \ldots\}$. Fig. 4 gives the calculated values of φ_{sep} measured from the rear stagnation point. They are in good agreement with the calculations of Fornberg [13] and of Dennis and Chang [11]. Theory based on the Helmholtz-Kirchhoff model predicts that as Re goes to infinity [1], the separation point may move forward to an angle of 125°. In [10] this angle is $\varphi = 1.815(104°)$. Our results and this possible limit are shown in Fig. 4.

ACKNOWLEDGEMENTS. This work was partially supported by the National Science Foundation of Bulgaria under Grant MM-610/96.

REFERENCES

1. Brodetsky, S. A proposal concerning laminar wakes behind bluff bodies at large Reynolds number. *Proc. Roy. Soc. A*, **102**, 1923, 542.
2. Christov, C. I. Orthogonal coordinate meshes with manageable Jacobian. In: *Numerical Grid Generation*, Joe F. Thompson ed., Elsevier, 1982, 885–894.
3. Christov, C. I. A Method for Treating the Stochastic Bifurcation of Plane Poiseuille flow. *Ann. l'Univ. Sof., Fac. Math. Mech.*, **76**, 2, Mécanique, 1982, 87–113.
4. Christov, C. I. A method for identification of homoclinic trajectories. In: *Proc. 14th Spring Conf. Union of Bulg. Mathematicians, Sunny Beach*, 1985, 571–577.
5. Christov, C. I. The method of variational imbedding for parabolic incorrect problems of coefficient identification. *Comp. Rend. Acad. Bulg. Sci.*, **40**(2), 1987, 21–24.
6. Christov, C. I. The method of variational imbedding for time reversal incorrect parabolic problems. *Comp. Rend. Acad. Buld. Sci.*, **40**(6), 1987, 5–8.
7. Christov, C. I. Gaussian elimination with pivoting for multidiagonal systems. *University of Reading, Internal Report* 4, 1994.
8. Christov, C. I., R. Marinova. Numerical Investigation of High Re Stationary Viscous Flow around Circular Cylinder as Inverse Problem. *Bulg. J. Meteorology Hydrology*, **5**, N. 3-4, 1994, 105–118.
9. Christov, C. I., J. Pontes, D. Walgraef, M. G. Velarde. Implicit time splitting for fourth-order Parabolic Equations. *Comp. Methods in Appl. Mech. Engn.*, 1997 (to appear).
10. Christov, C. I., M. D. Todorov. An inviscid model of flow separation around blunt bodies. *Compt. Rend. Acad. Bulg. Sci.*, **40**(7), 1987, 43–46.
11. Dennis, S. C. R., Gau-Zu Chang. Numerical solutions for steady flow past a circular cylinder at Reynolds numbers up to 100. *J. Fluid Mech.*, **42**(3), 1970, 471–489.
12. Douglas, J., H. H. Rachford. On the Numerical Solution of Heat Conduction Problems in Two and Three Space Variables. *Trans. Amer. Math. Soc.*, **82**, 1956, 421–439.
13. Fornberg, B. A numerical study of steady viscous flow past a circular cylinder. *J. Fluid Mech.*, **98**, 1980, 819-835.
14. Fornberg, B. Steady flow past a circular cylinder up to Reynolds number 600. *J. Comput. Phys.*, **61**, 1985, 297–320.

15. Fornberg, B. Steady incompressible flow past a row of circular cylinders. *J. Fluid Mech.*, **225**, 1991, 655–671.
16. Marinova, R. S. Identification of the Unstable Stationary Solutions of Navier-Stokes Equations at High Reynolds Numbers. In: *Continuum Models and Discrete Systems, Proc. 8^{th} Int. Symposium*, K. Z. Markov, ed., World Sci., 1996, 452–460.
17. Peregrine, D. H. A note on steady high-Reynolds-number flow about a circular cylinder. *J. Fluid Mech.*, **157**, 1985, 493–500.
18. Smith, F. T. Laminar flow of an incompressible fluid past a bluff body: the separation, reattachment, eddy properties and drag. *J. Fluid Mech.*, **92**, 1979, 171–205.
19. Smagulov, Sh., C. I. Christov. Iterationless numerical implementation of the boundary conditions in the vorticity-stream function formulation of Navier-Stokes equations. *Inst. of Theor. and Applied Mech.*, Novosibirsk, USSR, Preprint No 20, 1980, 21 p. (in Russian).
20. Smith, F. T. A structure for laminar flow past a bluff body at high Reynolds number. *J. Fluid Mech.*, **155**, 1985, 175–191.
21. Takami, H., H. B. Keller. Steady two–dimensional viscous flow of an incompressible fluid past a circular cylinder. *Phys. Fluids Suppl.* II, **51**, 1969.
22. Yanenko, N. N. Method of Fractional Steps. Gordon and Breach, London, 1971.

Received on June 20, 1997
Revised on August 20, 1997

Christo I. Christov
National Institute of Meteorology and Hydrology
Bulgarian Academy of Sciences
BG-1184 Sofia, Bulgaria
E-mail: christo.christov@meteo.bg

Rossitza S. Marinova
Department of Mathematics
Technical University of Varna
BG-9010 Varna, Bulgaria
E-mail: marinov@ms3.tu-varna.acad.bg